Can strong gravitational lensing constrain dark energy?

Seokcheon Lee[1] and Kin-Wang Ng[1,2]

[1]*Institute of Physics, Academia Sinica, Taipei, Taiwan 11529, Republic of China*
[2]*Institute of Astronomy and Astrophysics, Academia Sinica, Taipei, Taiwan 11529, Republic of China*

We discuss the ratio of the angular diameter distances from the source to the lens, D_{ds}, and to the observer at present, D_s, for various dark energy models. It is well known that the difference of D_ss between the models is apparent and this quantity is used for the analysis of Type Ia supernovae. However we investigate the difference between the ratio of the angular diameter distances for a cosmological constant, $(D_{ds}/D_s)^\Lambda$, and that for other dark energy models, $(D_{ds}/D_s)^{other}$, in this paper. It has been known that there is lens model degeneracy in using strong gravitational lensing. Thus, we investigate the model independent observable quantity, Einstein radius (θ_E), which is proportional to both D_{ds}/D_s and velocity dispersion squared, σ_v^2. D_{ds}/D_s values depend on the parameters of each dark energy model individually. However, $(D_{ds}/D_s)^\Lambda - (D_{ds}/D_s)^{other}$ for the various dark energy models, is well within the error of σ_v for most of the parameter spaces of the dark energy models. Thus, a single strong gravitational lensing by use of the Einstein radius may not be a proper method to investigate the property of dark energy. However, better understanding to the mass profile of clusters in the future or other methods related to arc statistics rather than the distances may be used for constraints on dark energy.

I. INTRODUCTION

Recent observations of high redshift Type Ia supernovae (SNe Ia) suggested that the expansion of the Universe is currently accelerating [1]. The cosmic microwave background (CMB) anisotropy data, indicating a spatially flat universe [2] containing a low value for the cold dark matter (CDM) density parameter [3], has confirmed that the Universe is dominantly made up of a component with negative pressure (dark energy) to make up the critical density today.

The cosmological constant and/or a quintessence field are the most commonly accepted candidates for dark energy. Although the cosmological constant is simple and favored by current cosmological observations, there is 50 to 120 orders of magnitude discrepancy between theory and the measured value [4]. The quintessence, which might alleviate this problem is a dynamical scalar field leading to a time dependent equation of state parameter [5]. Various scalar field potentials for the quintessence have been investigated [6].

It is important to use various ways of checking for the existence of dark energy in addition to SNe Ia and CMB anisotropy constraints on dark energy. A number of other tests have been considered including "geometric" tests using standard cosmological methods (the galaxy cluster gas mass fraction [7], the location of CMB peaks [8,9], the redshift-angular size [10], the strong gravitational lensing [11–14], fluctuations of the luminosity distance [15], etc.).

The statistics of gravitational lensing of quasars (QSOs) by intervening galaxies can constrain on the cosmological constant [12]. Lensed images of distant galaxies in cluster, arcs or rings, may provide a bound on the equation of state parameter of dark energy [13]. While SNeIa is used to

determine the luminosity distance itself, a gravitational lensing system can be used to measure the ratio of angular diameter distances. Thus, the gravitational lensing system is regarded as an independent tool that complements SNe Ia as a probe of dark energy [14].

However, the lensing observations primarily depend on the parameters of lens models with minor dependence on cosmological parameters [16]. There is the lens model degeneracy in both the projected mass density profile and the circular velocity profile. It is shown that we need to measure the Einstein radius and the velocity dispersion within $\mathcal{O}(1)\%$ accuracy in order to put a constraint on ω_{DE}.

In the gravitational lensing, one of the observable quantities without having any model dependence is the Einstein radius (θ_E), which is proportional to the velocity dispersion squared (σ_v^2) and the ratio of the angular distances D_{ds}/D_s, where D_{ds} is the distance from the lens to the source and D_s is that from the source to the observer. With different values of cosmological parameters, we can have different values of D_{ds}/Ds, i.e. different values of θ_E. Thus, it might be used for probing the property of dark energy, ω_{DE}. However, there is an ambiguity in measuring σ_v. If the error of σ_v measurement is not within the differences of D_{ds}/Ds between different cosmological models, then we cannot distinguish the differences between models by measuring θ_E.

This paper is organized as follows. In the next section we review the gravitational lensing system with the basic equations used in lensing observations. We also briefly mention the most popular lens models. We review the various aspects of errors in the modeling lens in Sec. III. In Sec. IV, we check both the differences of D_s and the differences of D_{ds}/Ds between the cosmological constant

043518-1

and other dark energy models. Our conclusion is in the last section.

II. GRAVITATIONAL LENSING AND ISOTHERMAL GALAXY MODELS

Figure 1 shows a simple lensing system [17]. Consider the source sphere S_s, i.e. a sphere with radius D_s, centered at the observer O and the deflector sphere S_d with radius D_d, i.e. the distance to the center of the lens L. In addition, consider the observer sphere S_o where the source would have angular position $\boldsymbol{\beta}$ (bold faced characters represent 2-dimensional vectors in this manuscript) if the light rays from the source S were not influenced by the gravitational field of the deflector. However, since light rays are bent by the lens, the straight line SO is no longer a physical ray path. Rather, there are light rays which connect the source and the observer but they are curved near S_d. One such ray $SI'O$ is drawn, together with its approximation SIO, consisting of the two asymptotes of the real ray. The separation of the light ray from the optical axis, LI, is defined as the impact vector $\boldsymbol{\xi}$ in the lens plane. The angle $\hat{\boldsymbol{\alpha}}$ between the two asymptotes SI and IO is the deflection angle caused by the matter distribution L,

$$\hat{\boldsymbol{\alpha}} = 4G \int_{R^2} \Sigma(\boldsymbol{\xi}') \frac{\boldsymbol{\xi} - \boldsymbol{\xi}'}{|\boldsymbol{\xi} - \boldsymbol{\xi}'|^2} d^2\boldsymbol{\xi}', \qquad (2.1)$$

where the integral is over the lens plane and $\Sigma(\boldsymbol{\xi}')$ is the surface matter density at position $\boldsymbol{\xi}'$ resulting from the projection of the volume mass distribution of the deflector onto the lens plane. This is valid when the gravitational field is weak, hence the deflection angle is small. The observer will thus see the source at the position $\boldsymbol{\theta}$ on his sphere S_o.

From the geometry of Fig. 1, we can easily derive a relation between the source position described by the unlensed position angle $\boldsymbol{\beta}$ and the position of the images $\boldsymbol{\theta} = \boldsymbol{\xi}/D_d$ of the source

$$\boldsymbol{\beta} = \boldsymbol{\theta} - \frac{D_{ds}}{D_s} \hat{\boldsymbol{\alpha}}(\boldsymbol{\xi}). \qquad (2.2)$$

We can reexpress this equation by using the distance $\boldsymbol{\eta} = D_s\boldsymbol{\beta}$ from the source to the optical axis as

$$\boldsymbol{\eta} = \frac{D_s}{D_d} \boldsymbol{\xi} - D_{ds}\hat{\boldsymbol{\alpha}}(\boldsymbol{\xi}). \qquad (2.3)$$

It is useful to rewrite lens equations (2.2) and (2.3) in dimensionless form by introducing a length scale ξ_0 in the lens plane, which is called the Einstein radius in the lens plane and a corresponding length scale $\eta_0 = \xi_0 D_s/D_d$ in the source plane. The Einstein radius in the lens plane is given by

$$\xi_0 = \sqrt{4GM_d} \cdot \sqrt{\frac{D_d D_{ds}}{D_s}}, \qquad (2.4)$$
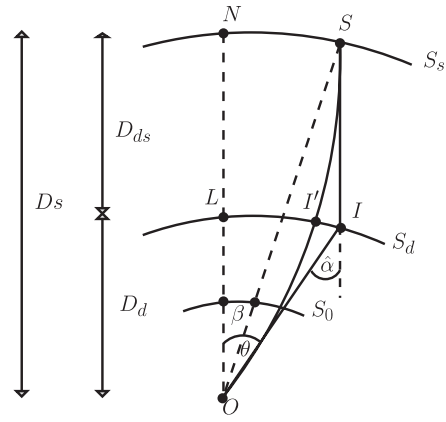

FIG. 1. A general lensing system. L is the center of the lens, and the line through L and the observer O is the optical axis. $\boldsymbol{\beta}$ is an unperturbed angular position of the source relative to that. $\hat{\boldsymbol{\alpha}}$ is the deflection angle of a light ray, thus an image of the source is observed at position $\boldsymbol{\theta}$. However all angles are very small; we can replace the real light ray ($SI'O$) by its approximation SIO.

where M_d is the mass of the lensing object. By use of the definition of the dimensionless vectors $\boldsymbol{x} \equiv \boldsymbol{\xi}/\xi_0$ and $\boldsymbol{y} \equiv \boldsymbol{\eta}/\eta_0$ as well as the dimensionless surface mass density (convergence) $\kappa(\boldsymbol{x}) = \Sigma(\xi_0 \boldsymbol{x})/\Sigma_{\rm cr}$ where the critical surface matter density $\Sigma_{\rm cr} = \frac{1}{4\pi G} \frac{D_s}{D_d D_{ds}}$, the lens equations are rewritten as

$$\boldsymbol{y} = \boldsymbol{x} - \boldsymbol{\alpha}(\boldsymbol{x}) = \boldsymbol{x} - \frac{m(\boldsymbol{x})}{\boldsymbol{x}}, \qquad (2.5)$$

where α is the scaled deflection angle,

$$\boldsymbol{\alpha}(\boldsymbol{x}) = \frac{D_d D_{ds}}{D_s \xi_0} \hat{\boldsymbol{\alpha}}(\xi_0 \boldsymbol{x}) = \frac{1}{\pi} \int_{R^2} d^2\boldsymbol{x}' \kappa(\boldsymbol{x}') \frac{\boldsymbol{x} - \boldsymbol{x}'}{|\boldsymbol{x} - \boldsymbol{x}'|^2}, \qquad (2.6)$$

and $m(\boldsymbol{x})$ is defined as

$$m(\boldsymbol{x}) = 2 \int_0^x \kappa(\boldsymbol{x}') \boldsymbol{x}' d\boldsymbol{x}'. \qquad (2.7)$$

If the lensing object is a point mass, then the cross section σ for strong lensing events is given by [18]

$$\sigma = \pi \xi_0^2. \qquad (2.8)$$

We need to specify the mass distribution Σ to solve the lens equation (2.5). One simple and analytic solution of a differential equation for the radial mass distribution is the singular isothermal sphere (SIS) [18]. Its surface mass density, projected onto the lens plane, is given by

$$\Sigma(\boldsymbol{\xi}) = \frac{\sigma_v^2}{2G} \frac{1}{\xi}, \qquad (2.9)$$

where σ_v is the velocity dispersion along the line of sight and the length scale $\xi_0 = 4\pi \sigma_v^2 \frac{D_d D_{ds}}{D_s}$. With these we get the lens equation

$$y = x - \frac{x}{|x|}, \qquad (2.10)$$

with the convergence

$$\kappa(x) = \frac{1}{2x}. \qquad (2.11)$$

Because of its simplicity and the consistency with the matter distribution of galaxies, the SIS is frequently used as the gravitational lens model. In addition to SIS, a non-singular isothermal sphere (NIS), the singular isothermal ellipsoid (SIE), and Navarro-Frenk-White (NFW) [19] are the most commonly used gravitational lens models. All of them are distinguished by their own surface mass densities as in Eq. (2.9).

III. ERRORS IN THE MODELING LENS

In this section we review systematic errors in the ratio D_{ds}/D_s [14]. As we mentioned in the previous section, the various isothermal galaxy models are specified by their surface mass densities (Σ), which are the function of the velocity dispersion (σ_v) along the line of sight. Isothermal ellipsoid models (SIE, NIE) have an additional necessary measurement, the ratio f of the minor axis to the major axis, $\zeta = \sqrt{\xi_1^2 + f^2 \xi_2^2}$, which is related to the ellipticity ϵ by

$$f = \sqrt{(1 + \epsilon)/(1 - \epsilon)}. \qquad (3.1)$$

The lens equation gives an elliptical image of the Einstein ring with the minor and major axes

$$\theta_{\pm} = \theta_E \sqrt{1 \pm \epsilon}, \qquad (3.2)$$

where

$$\theta_E = 4\pi \sigma_v^2 \frac{D_{ds}}{D_s}, \qquad (3.3)$$

as given in Eq. (2.4). Thus D_{ds}/D_s can be determined by measuring σ_v, f, and θ_E.

Even though gravitational lensing has been used as a useful cosmological tool to probe the high redshift universe, there are several problems. Observational quantities depend on a lens model, which has inherent uncertainties in itself [20]. In most cases, we do not know the property of the lensing object in detail. Also, the light propagates through the local inhomogeneous spacetime which deviates from the smoothed Robertson-Walker metric. Thus, even though the global parameters such as the energy density parameters are fixed, the distance formula is not uniquely determined [21]. In spite of all these ambiguities, if dark energy dominates over the mass density, then the optical depth increases dramatically and its effect is much larger than the uncertainty arising from the problems in the formulation [22]. However in the following section we investigate the model independent observable quantity, Einstein radius.

IV. ANGULAR DIAMETER DISTANCES

In this section, we investigate the ratio of the angular diameter distances from the lens to the sources (D_{ds}) and those from the source to the present observer (D_s) for various dark energy models. We consider a spatially flat, homogeneous, and isotropic universe with radiation, matter, and dark energy.

The angular diameter distance from the observer at present to the source, $D_s(0, z_s)$, is defined as

$$D_s(0, z_s) = \frac{d(0, z_s)}{\delta} = d_L(1 + z_s)^{-2} = a_s r_s = \frac{D(0, z_s)}{(1 + z_s)}$$

$$= \frac{H_0^{-1}}{(1 + z_s)} \int_0^{z_s} \frac{dz}{\sqrt{\Omega_m^{(0)}(1 + z)^3 (1 + \frac{(1+z)}{(1+z_{eq})}) + \Omega_{DE}^{(0)} e^{3 \int_0^z (1 + \omega_{DE}) d\ln(1+z')}}}, \qquad (4.1)$$

where d_L is the luminosity distance and z_{eq} is the redshift when radiation and matter densities are equal. In the following numerical calculations, we use $a_{eq} = (1 + z_{eq})^{-1} = 1/5510$. The angular diameter distance depends on the present values of energy density contrast of matter ($\Omega_m^{(0)}$) and dark energy ($\Omega_{DE}^{(0)}$) and the equation of state of dark energy (ω_{DE}) as in Eqs. (4.1) and (4.2). In a flat universe, we have the constrain $\Omega_m^{(0)} + \Omega_{DE}^{(0)} \simeq 1$ when we use the fact that $\Omega_r^{(0)} \ll \Omega_m^{(0)}, \Omega_{DE}^{(0)}$. Especially, dark energy is the cosmological constant (Λ) when $\omega_{DE}^{(0)} =$

−1.0 and we call the model including cold dark matter and cosmological constant the ΛCDM model.

However $H_0 D_s$ itself may not be an interesting quantity in the study of gravitational lensing. Instead, we need to know the combination of angular diameter distances. We want to investigate the least model dependent observable quantity for our study and Einstein radius is one of the proper objects for this purpose. We can represent the angular diameter distance from the lens to the source as

$$D_{ds}(z_d, z_s) = \frac{H_0^{-1}}{(1 + z_s)} \int_{z_d}^{z_s} \frac{dz}{\sqrt{\Omega_m^{(0)}(1 + z)^3(1 + \frac{(1+z)}{(1+z_{eq})}) + \Omega_{DE}^{(0)} e^{3 \int_0^z (1+\omega_{DE}) d \ln(1+z')}}}, \quad (4.2)$$

where we assume $z_s > z_d$.

If we rewrite the Einstein radius, Eq. (3.3), then the ratio of the angular diameter distances D_{ds}/D_s is given by

$$R_{ds} \equiv \frac{D_{ds}}{D_s} = \frac{\theta_E}{4\pi\sigma_v^2}, = \frac{\int_{z_d}^{z_s} \frac{dz}{\sqrt{\Omega_m^{(0)}(1+z)^3(1+((1+z)/(1+z_{eq})))+\Omega_{DE}^{(0)} \exp(3 \int_0^z (1+\omega_{DE})d \ln(1+z'))}}}{\int_0^{z_s} \frac{dz}{\sqrt{\Omega_m^{(0)}(1+z)^3(1+((1+z)/(1+z_{eq})))+\Omega_{DE}^{(0)} \exp(3 \int_0^z (1+\omega_{DE})d \ln(1+z'))}}}. \quad (4.3)$$

Thus, the error that contributes to this ratio due to the error from the velocity dispersion is

$$\left| \frac{\Delta R_{ds}}{R_{ds}} \right| = 2 \frac{\Delta \sigma_v}{\sigma_v}. \quad (4.4)$$

We will not consider any detail of the lens model, which can cause to arise additional errors. From various sources of the lens system, we can roughly say that the error of the velocity dispersion is about 5% ($\Delta\sigma_v/\sigma_v \sim 5\%$) [23]. That means we can distinguish the differences between models if the difference of the ratio of the angular diameter distances between models, $\Delta R_{ds}/R_{ds}$ is at least 5%. Now we will compare the differences of the ratios of angular diameter distances for different models. There was a work related to this approach [24]. However in the previous work, the equation of state parameter of dark energy was constrained as a constant. We consider more general cases with the stronger constraint on constant ω_{DE}s.

A. R_{ds} when $\omega_{DE} = \text{constant}$

We assume that the stand cosmological parameters are $\Omega_{DE}^{(0)} = 0.73$ and $\omega_{DE}^{(0)} = -1.0$ and we denote the ratio of the angular diameter distances D_{ds}/D_s with these parameters as R_{ds}^Λ. Figure 2 shows the difference of R_{ds} between the standard case and the various constant equation of state

cases, $\Delta^{\text{const}} \equiv |R_{ds}^\Lambda - R_{ds}^{\text{const}}|/R_{ds}^\Lambda \times 100(\%)$. In the left panel of Fig. 2, we show the Δ^{const} dependence on $\Omega_{DE}^{(0)}$ for different values of $\omega_{DE}^{(0)}$, -1.0 (solid line), -0.8 (dotted line), and -0.5 (dash-dotted line). If there is an error in measuring $\Omega_{DE}^{(0)}$ within the range $0.51 \leq \Omega_{DE}^{(0)} \leq 0.87$ ($0.52 \leq \Omega_{DE}^{(0)} \leq 0.89$, $0.57 \leq \Omega_{DE}^{(0)}$) for $\omega_{DE}^{(0)} = -1.0(-0.8, -0.5)$, then Δ^{const} is less than 5%. For example, if the measured cosmological parameters are $\omega_{DE}^{(0)} = -0.5$ and $\Omega_{DE}^{(0)} \geq 0.57$, then we cannot distinguish this with the standard case ($\omega_{DE}^{(0)} = -1.0$ and $\Omega_{DE}^{(0)} = 0.73$) within 5% by using R_{ds}, i.e. by measuring θ_E. $\Omega_{DE}^{(0)}$ also varies for different values of ω_{DE}, so $\omega_{DE}^{(0)} = -1.0$ does not necessarily have a smaller difference to the standard case as can be shown in the left panel of Fig. 2. When $\omega_{DE}^{(0)} = -1.0$, we can have the standard case if $\Omega_{DE}^{(0)} = 0.73$. In this case $\Delta^{\text{const}} = 0$. This is shown in the left panel of Fig. 2 and it shows the consistency of figures. We show Δ^{const} dependence on $\omega_{DE}^{(0)}$ for different values of $\Omega_{DE}^{(0)}$, 0.85 (solid line), 0.73 (dotted line), and 0.60 (dash-dotted line) in the right panel of Fig. 2. Again if there is an error in measuring $\omega_{DE}^{(0)}$ within the range $\omega_{DE}^{(0)} \leq -0.23$ ($-0.30, -0.44$) for $\Omega_{DE}^{(0)} = 0.85$ (0.73, 0.60), then Δ^{const} is less than 5%. For example, if the measured cosmological parameters are $\Omega_{DE}^{(0)} = 0.85$
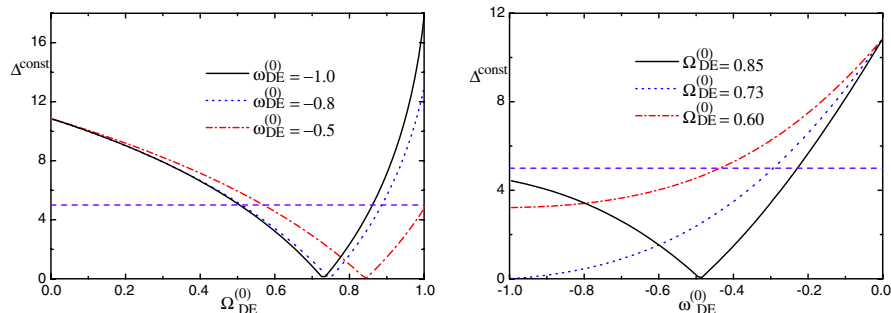

FIG. 2 (color online). The ratio of angular diameter distances Δ^{const} for the constant equation of state of dark energy (ω_{DE}). (a) Dependence on the present value of dark energy density contrast $\Omega_{DE}^{(0)}$ of Δ^{const} for different present values of equation of state of dark energy $\omega_{DE}^{(0)}$: -1.0 (solid line), -0.8 (dotted line), and -0.5 (dash-dotted line), respectively. (b) Dependence on the value of $\omega_{DE}^{(0)}$ of Δ^{const} for different values of $\Omega_{DE}^{(0)}$: 0.85 (solid line), 0.73 (dotted line), and 0.60 (dash-dotted line), respectively.
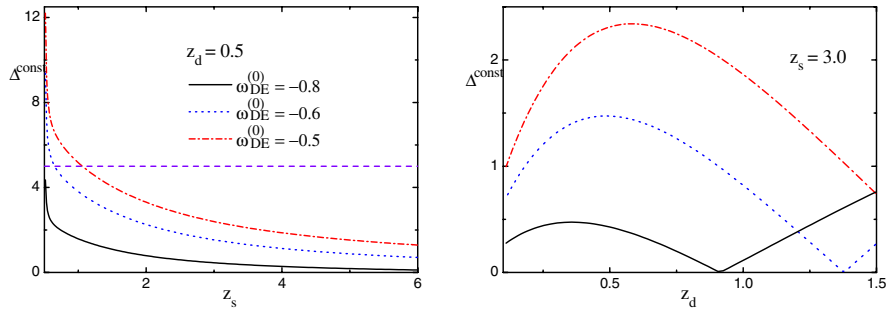
FIG. 3 (color online). Δ^{const} for the constant ω_{DE} as a function of the location of the source (z_s). (a) Dependence on the position of the source (z_s) of Δ^{const} for different values of $\omega_{\mathrm{DE}}^{(0)}$, with the same notation for the label as the left panel of Fig. 2 when $\Omega_{\mathrm{DE}}^{(0)} = 0.73$. (b) Dependence on the position of the lens (z_d) of Δ^{const} for different present values of $\omega_{\mathrm{DE}}^{(0)}$, with the same notation as the left panel.

and $\omega_{\mathrm{DE}}^{(0)} \leq -0.23$, then we cannot distinguish this with the standard case within 5%. We can also see that $\Delta^{\mathrm{const}} = 0$ when $\Omega_{\mathrm{DE}}^{(0)} = 0.73$ and $\omega_{\mathrm{DE}}^{(0)} = -1.0$ in the right panel of Fig. 2.

We show the dependence of Δ^{const} on the position of source (z_s) in the left panel of Fig. 3 for different values of $\omega_{\mathrm{DE}}^{(0)}$ -0.8 (solid line), -0.6 (dotted line), and -0.5 (dash-dotted line). We choose the position of the lens as $z_d = 0.5$ and $\Omega_{\mathrm{DE}}^{(0)} = 0.73$. If we choose $z_s = 3.0$ for different values of $\omega_{\mathrm{DE}}^{(0)}$, then we have the same values of Δ^{const} of the dotted line of the right panel of Fig. 2. If the source position of the lensing system is located $z_s \gtrsim 0.64$ (1.04) for $\omega_{\mathrm{DE}}^{(0)} = -0.6$ (-0.5), then Δ^{const} is less than 5%. We cannot distinguish the difference of R_{ds}s between the standard case and $\omega_{\mathrm{DE}}^{(0)} = -0.8$ within 5% independent of the source position. In the right panel of Fig. 3, we show the dependence of Δ^{const} on the position of the lens (z_d) when we choose $z_s = 3.0$ and $\Omega_{\mathrm{DE}}^{(0)} = 0.73$ with the same notation as the left panel of the figure for the different values of $\omega_{\mathrm{DE}}^{(0)}$. When we vary z_d from 0.1 to 1.5 for every value of $\omega_{\mathrm{DE}}^{(0)}$ ($-0.8 \leq \omega_{\mathrm{DE}}^{(0)} \leq -0.5$), Δ^{const}s are well below 5%. To check the consistency between the figures, we can check Δ^{const} values when we choose $z_d = 0.5$ in the right panel of Fig. 2. This gives $\Delta^{\mathrm{const}} \simeq 0.44$ (1.5, 2.3) when $\omega_{\mathrm{DE}}^{(0)} =$

$-0.8(-0.6, -0.5)$, which is equal to Δ^{const} value when we choose $z_s = 3.0$ in the left panel of the same figure.

B. R_{ds} when $\omega_{\mathrm{DE}} = \omega_0 + \omega_1(1 - a)$

Now we check the difference of the ratio of the angular diameter distances D_{ds}/D_s between the standard case and one of the time varying ω_{DE} models, $\omega_{\mathrm{DE}} = \omega_0 + \omega_1(1 - a)$ [25]. We define $\Delta^{\mathrm{p}} \equiv |R_{ds}^{\Lambda} - R_{ds}^{\mathrm{p}}|/R_{ds}^{\Lambda} \times 100(\%)$ where R_{ds}^{p} means R_{ds} value when we use $\omega_{\mathrm{DE}} = \omega_0 + \omega_1(1 - a)$. We assume that there is no error in the measured value of $\Omega_{\mathrm{DE}}^{(0)} = 0.73$ in this case. We show Δ^{p} dependence on ω_0 value for different values of ω_1, 0.3 (solid line), 0.2 (dotted line), and 0.1 (dash-dotted line), respectively, in the left panel of Fig. 4. Δ^{p} is within 5% for $\omega_1 = 0.3$ (0.2, 0.1) when $\omega_0 \leq -0.43$ ($-0.38, -0.34$). For example, when $\omega_1 = 0.3$ and $\omega_0 \leq -0.43$, then we cannot distinguish the cosmology with the cosmological constant from the cosmological model with time varying dark energy $\omega_{\mathrm{DE}} = \omega_0 + \omega_1(1 - a)$ within 5% by using R_{ds}. In the right panel of Fig. 4, we show the ω_1 dependence of Δ^{p} for different values of ω_0, -1.0 (solid line), -0.9 (dotted line), and -0.8 (dash-dotted line). When ω_1 varies from 0 to 1 every Δ^{p} value is within 5% for every value of ω_0 from -1.0 to -0.8. For the consistency check we can choose $\omega_1 = 0.3$ for three different lines. We can check these values with the
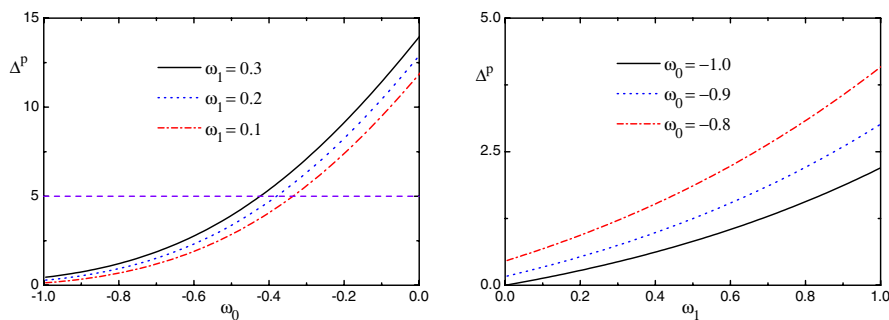

FIG. 4 (color online). Δ^{p} for the time varying equation of state of dark energy ($\omega_{\mathrm{DE}} = w_0 + w_1(1 - a)$). (a) Dependence on the value of ω_0 for different values of ω_1: 0.1 (solid line), 0.2 (dotted line), and 0.3 (dash-dotted line), respectively. (b) Dependence on the value of ω_1 of Δ^{p} for different values of ω_0: -1.0 (solid line), -0.9 (dotted line), and -0.8 (dash-dotted line), respectively.
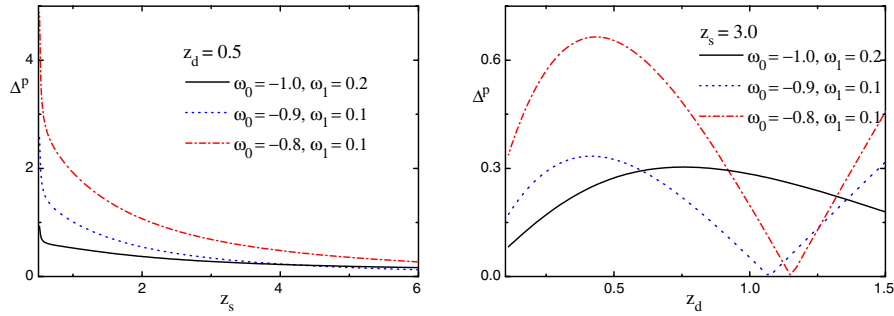
FIG. 5 (color online). Δ^{p}. (a) Dependence on z_s of Δ^{p} for various sets of ω_0 and ω_1. (b) Dependence on z_d of Δ^{p} for the same sets of ω_0 and ω_1 as in the left panel.

three different points of solid line of the left panel of the figure. When we choose $\omega_1 = 0.3$, $\Delta^{\mathrm{p}} = 0.450.76$, and 1.2 for $\omega_0 = -1.0$, -0.9, and -0.8 in both the left and right panels of Fig. 4.

We again check Δ^{p} dependence on the position of z_s and z_d for the various sets of ω_0 and ω_1 values in Fig. 5. In the left panel of Fig. 5, we show Δ^{p} dependence on z_s. We choose $z_d = 0.5$ and $\Omega_{\mathrm{DE}}^{(0)} = 0.73$ in this case. For the given sets of ω_0 and ω_1 values, we cannot distinguish the cosmological model with the cosmological constant from the cosmological model with time varying dark energy $\omega_{\mathrm{DE}} = \omega_0 + \omega_1(1 - a)$ no matter where the source of the lens is located from $z_s = 0.5$ to 6 within 5% by measuring R_{ds}. We check z_d dependence on Δ^{p} for the same sets of ω_0 and ω_1 in the right panel of Fig. 5. We choose $z_s = 3.0$. Again none of the case can be distinguished with the cosmological constant case within 5%.

C. R_{ds} when $\omega_{\mathrm{DE}} = -1 + 4a_c^q/3(a^q + a_c^q)$

We check another time varying dark energy model by using the parameter $\omega_{\mathrm{DE}} = -1 + 4a_c^q/3(a^q + a_c^q)$ in Fig. 6. We define $\Delta^{\mathrm{SL}} \equiv |R_{ds}^{\Lambda} - R_{ds}^{\mathrm{SL}}|/R_{ds}^{\Lambda} \times 100(\%)$ where R_{ds}^{SL} means R_{ds} value when we use $\omega_{\mathrm{DE}} = -1 + 4a_c^q/3(a^q + a_c^q)$ [6]. The angular diameter distance of this parametrization is almost degenerate with that of the cosmological constant. Thus, the ratio difference of angular diameter distances between this parametrization and the

cosmological constant is extremely small for the different choice of parameters. We choose $\Omega_{\mathrm{DE}}^{(0)} = 0.73$, $z_s = 3.0$, and $z_d = 0.5$ in this figure. In the left panel of Fig. 6, we show the dependence of Δ^{SL} on q for the different values of x_c, -2.00 (solid line), -2.64 (dotted line), and -3.00 (dash-dotted line). For all of the cases, Δ^{SL} are within 1% for different values of x_c from $q = 2$ to 5. In the right panel of Fig. 6, we show Δ^{SL} dependence on x_c for different values of q, 1 (solid line), 3 (dotted line), and 5 (dash-dotted line). Except for the $q = 1$ case, Δ^{SL} are degenerate within 1%. Thus, we cannot tell any difference between the cosmological constant and the dark energy with the parameter $\omega_{\mathrm{DE}} = -1 + 4a_c^q/3(a^q + a_c^q)$ by measuring R_{ds} within 5%.

We again check Δ^{SL} dependence on the position of z_s and z_d for various sets of x_c and q values in Fig. 7. In the left panel of Fig. 7, we show Δ^{SL} dependence on z_s. We choose $z_d = 0.5$ and $\Omega_{\mathrm{DE}}^{(0)} = 0.73$ in this case. For given sets of (x_c, q) values, $(-2.00, q = 4)$ (solid line), $(-2.64, q = 3)$ (dotted line), and $(-3.00, q = 2)$ (dash-dotted line), we cannot distinguish the cosmological model with the cosmological constant from the cosmological model with time varying dark energy $\omega_{\mathrm{DE}} = -1 + 4a_c^q/3(a^q + a_c^q)$ no matter where the source of the lens is located from $z_s = 0.5$ to 6 within 1% by measuring R_{ds}. We check z_d dependence on Δ^{SL} for the same sets of x_c and q in the left panel of the figure. We choose $z_s = 3.0$. Again
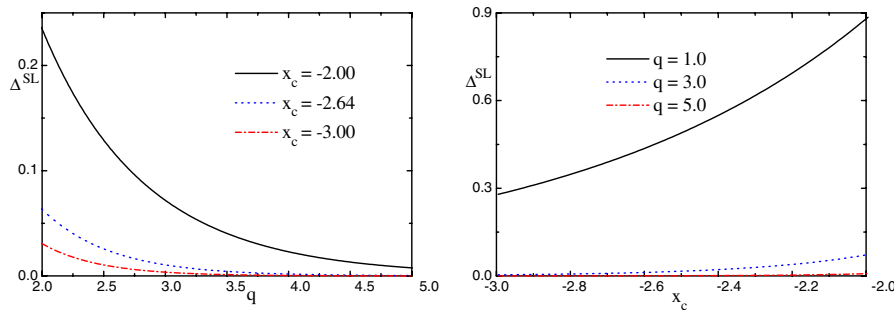

FIG. 6 (color online). Δ^{SL} for the varying equation of state of dark energy ($\omega_{\mathrm{DE}} = -1 + 4a_c^q/3(a^q + a_c^q)$). (a) Dependence on q of Δ^{SL} for different values of x_c: -2.00 (solid line), -2.64 (dotted line), and -3.00 (dash-dotted line), respectively. (b) Dependence on x_c of Δ^{SL} for different values of q: 1.0 (solid line), 3.0 (dotted line), and 5.0 (dash-dotted line), respectively.
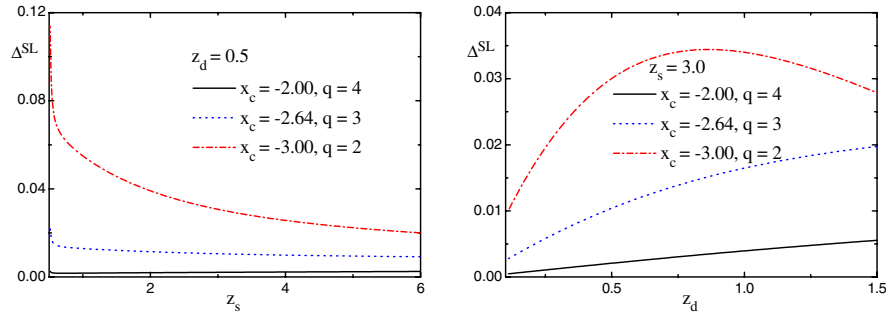
FIG. 7 (color online). Δ^{SL}. (a) Dependence on z_s of Δ^{SL} for various sets of x_c and q values. (b) Dependence on z_d of Δ^{SL} for the same sets of x_c and q values as in the left panel.

none of the cases can be distinguished from the cosmo-logical constant case within 1%.

V. CONCLUSIONS

We have investigated the angular diameter distances from the source to the present observer for the various dark energy models. The angular diameter distance is proportional to the luminosity distance, which is used for the analysis of Type Ia supernovae. The difference of $H_0 D_s$ between models is apparent and measuring this quantity as to probe dark energy models might be proper for further investigation. In addition to SNeIa, the gravitational lensing has been known as the possible method to probe the property of dark energy.

Most of the lensing analyses have the Einstein radius as a basic quantity. This is the lens model independent ob-servable quantity and might be a good probe for the prop-erty of dark energy. The Einstein radius is proportional to both the ratio of the angular diameter distances and the velocity dispersion squared. However, we have shown that there is degeneracy between different models for the value of the ratio of the angular diameter distances. If the error in measuring the velocity dispersion exceeds the difference of the ratio of the angular diameter distances of two different dark energy models, then we cannot distinguish the differ-ences between different dark energy models by measuring the Einstein radius. In our analysis we have shown that this is the case for most of the parameter spaces of the dark energy models. Thus, a single strong gravitational lensing might not be a proper method to investigate the property of dark energy. However, better understanding to the mass profile of clusters in the future or other methods related to arc statistics rather than the distances may be still used for constraints on dark energy.

[1] A. G. Riess *et al.* (Supernova Search Team Collaboration), Astron. J. **116,** 1009 (1998); Astrophys. J. **607,** 665 (2004); S. Perlmutter *et al.* (Supernova Cosmology Project Collaboration), Astrophys. J. **517,** 565 (1999); N. A. Bahcall, J. P. Ostriker, S. Perlmutter, and P. J. Steinhardt, Science **284,** 1481 (1999); T. Padmanabhan and T. R. Choudhury, Mon. Not. R. Astron. Soc. **344,** 823 (2003); Astron. Astrophys. **429,** 807 (2005); P. Astier *et al.*, arXiv:astro-ph/0510447.

[2] C. L. Bennett *et al.*, Astrophys. J. Suppl. Ser. **148,** 1 (2003); D. N. Spergel *et al.*, Astrophys. J. Suppl. Ser. **148,** 175 (2003); arXiv:astro-ph/0603449.

[3] M. Colless *et al.*, Mon. Not. R. Astron. Soc. **328,** 1039 (2001); arXiv:astro-ph/0306581; M. Tegmark *et al.*, Phys. Rev. D **69,** 103501 (2004).

[4] See, for example, S. Weinberg, Rev. Mod. Phys. **61,** 1 (1989).

[5] B. Ratra and P. J. E. Peebles, Phys. Rev. D **37,** 3406 (1988); Astrophys. J. **325,** L17 (1988); C. Wetterich, Nucl. Phys. **B302,** 668 (1988); R. R. Caldwell, R. Dave, and P. J. Steinhardt, Phys. Rev. Lett. **80,** 1582 (1998); P. G. Ferreira and M. Joyce, Phys. Rev. D **58,** 023503 (1998).

[6] See, for example, S. Lee, arXiv:astro-ph/0604602.

[7] S. Sasaki, Publ. Astron. Soc. Jpn. **48,** L119 (1996); U.-L. Pen, New Astron **2,** 309 (1997); S. W. Allen *et al.*, Mon. Not. R. Astron. Soc. **353,** 457 (2004); G. Chen and B. Ratra, Astrophys. J. **612,** L1 (2004); D. Puetzfeld, M. Pohl, and Z.-H. Zhu, Astrophys. J. **619,** 657 (2005); D. Rapetti, S. W. Allen, and J. Weller, Mon. Not. R. Astron. Soc. **360,** 555 (2005); Z. Chang, F.-Q. Wu, and X. Zhang, Phys. Lett. B **633,** 14 (2006); K. M. Wilson, G. Chen, and B. Ratra, arXiv:astro-ph/0602321.

[8] W. Hu, N. Sugiyama, and J. Silk, Nature (London) **386**, 37 (1997); W. Hu, M. Fukugita, M. Zaldarriaga, and M. Tegmark, Astrophys. J. **549**, 669 (2001); M. Doran, M. Lilley, J. Schwindt, and C. Wetterich, Astrophys. J. **559**, 501 (2001); M. Doran and M. Lilley, Mon. Not. R. Astron. Soc. **330**, 965 (2002); W. Lee and K.-W. Ng, Phys. Rev. D **67**, 107302 (2003); M. C. Bento, O. Bertolami, and A. A. Sen, Phys. Rev. D **67**, 063003 (2003); W. Hu, Ann. Phys. (N.Y.) **303**, 203 (2003); T. Barreiro, M. C. Bento, N. M. C. Santos, and A. A. Sen, Phys. Rev. D **68**, 043515 (2003).

[9] S. Lee, Phys. Rev. D **71**, 123528 (2005).

[10] G. Chen and B. Ratra, Astrophys. J. **582**, 586 (2003); S. Podariu, R. A. Daly, M. P. Mory, and B. Ratra, Astrophys. J. **584**, 577 (2003).

[11] M. Fukugita, T. Futamase, and M. Kasai, Mon. Not. R. Astron. Soc. **246**, 24 (1990); E. L. Turner, Astrophys. J. **365**, L43 (1990); B. Ratra and A. Quillen, Mon. Not. R. Astron. Soc. **259**, 738 (1992); L. F. Bloomfield Torres and I. Waga, Mon. Not. R. Astron. Soc. **279**, 712 (1996); I. Waga and J. A. Frieman, Phys. Rev. D **62**, 043521 (2000); Z.-H. Zhu, Mod. Phys. Lett. A **15**, 1023 (2000); T. Futamase and S. Yoshida, Prog. Theor. Phys. **105**, 887 (2001); G. Golse, J. P. Kneib, and G. Soucail, Astron. Astrophys. **387**, 788 (2002); N. Sarbu, D. Rusin, and C.-P. Ma, Astrophys. J. **561**, L147 (2001); K.-H. Chae, G. Chen, B. Ratra, and D.-W. Lee, Astrophys. J. **607**, L71 (2004); M. Jarvis, B. Jain, G. Bernstein, and D. Dolney, Astrophys. J. **644**, 71 (2006).

[12] C. S. Kochanek, Astrophys. J. **466**, 638 (1996).

[13] T. Futamase and T. Hamana, Prog. Theor. Phys. **102**, 1037 (1999).

[14] K. Yamamoto, Y. Kadoya, T. Murata, and T. Futamase, Prog. Theor. Phys. **106**, 917 (2001).

[15] C. Bonvin, R. Durrer, and M. A. Gasparini, Phys. Rev. D **73**, 023523 (2006); C. Bonvin, R. Durrer, and M. Kunz, Phys. Rev. Lett. **96**, 191302 (2006).

[16] T. Chiba and R. Takahashi, Prog. Theor. Phys. **107**, 625 (2002); N. Dalal, J. Hennawi, and P. Bode, Astrophys. J. **622**, 99 (2005).

[17] P. Schneider, J. Ehlers, and E. E. Falco, *Gravitational Lensing*, Astronomy and Astrophysics Series (Springer-Verlag, Berlin, 1992); P. Kormann, P. Schneider, and M. Bartelmann, Astron. Astrophys. **284**, 285 (1994).

[18] J. R. Gott and J. E. Gunn, Astrophys. J. **190**, L105 (1974); E. L. Turner, J. P. Ostriker, and J. R. Gott, Astrophys. J. **284**, 1 (1984).

[19] J. Navarro, C. S. Frenk, and S. D. M. White, Mon. Not. R. Astron. Soc. **275**, 720 (1995); M. Bartelmann, Astron. Astrophys. **313**, 697 (1996).

[20] F. Perrotta, C. Baccigalupi, M. Bartelmann, G. D. Zotti, and G. L. Granato, Mon. Not. R. Astron. Soc. **329**, 445 (2002); G. Golse, J. P. Kneib, and G. Soucail, Astron. Astrophys. **387**, 788 (2002); T. Chiba and R. Takahashi, Prog. Theor. Phys. **107**, 625 (2002).

[21] Y. Zel'dovich, Sov. Astron. **8**, 13 (1964); V. M. Dashevskii and V. I. Slysh, Sov. Astron. **9**, 671 (1966); C. C. Dyer and R. C. Roeder, Astrophys. J. **174**, L115 (1972); **180**, L31 (1973); T. Futamase and M. Sasaki, Phys. Rev. D **40**, 2502 (1989).

[22] M. Fukugita, T. Futamase, M. Kasai, and E. L. Turner, Astrophys. J. **393**, 3 (1992).

[23] J. L. Tonry and M. Frank, Astrophys. J. **515**, 512 (1999); K.-H. Chae, Astrophys. J. **630**, 764 (2005); A. B. Bolton *et al.*, Astrophys. J. **638**, 703 (2006); K.-H. Chae, S. Mao, X. Kang, and Y.-P. Jing, arXiv:astro-ph/0605405.

[24] M. Sereno, Astron. Astrophys. **393**, 757 (2002).

[25] E. V. Linder, Phys. Rev. D **70**, 023511 (2004).